

## MICRO-EARTHQUAKES OCCURRING IN THE VICINITY OF KYOTO (2)

By

Kennosuke OKANO and Isamu HIRANO

(Received November 18, 1965)

### Abstract

One of the conclusions drawn in the first paper that micro-earthquakes are very frequent in a belt-like region running from Wakasa Bay to Osaka Bay is strongly confirmed by use of data obtained after the publication of the first paper. According to the analysis of data, the focal depths of the micro-earthquakes are shallow in the east end of the belt-like region, and become deeper toward the west end. The deepest of focal depths, as was already pointed out, lie in the crust. For making the focal mechanism of the micro-earthquakes clear, the first motions of P waves are also examined. As a result, the distribution of the first motions of P waves is of quadrant type, and the horizontal component of the maximum pressure lie in the E-W direction, which agrees comparatively well with the direction of the maximum pressure of very shallow earthquakes occurring in Kinki District. The frequent occurrence of not only micro-earthquakes but the larger earthquakes in the belt-like region might have a close relation to the geologically distinctive features found in Bouguer anomaly, horizontal displacements and Quaternary faults. It is also shown that the region concerned, if uniform, has the mean velocity of 5.8 to 6.0km/sec for P, and 3.4 to 3.5km/sec for S.

### 1. Introduction

The routine observation of micro-earthquakes in the vicinity of Kyoto has shown that the micro-earthquakes frequently occur in the crustal part of a belt-like region running from Wakasa Bay to Osaka Bay (1964, Okano and Hirano). In the previous study, the arrival times of P waves at the four stations—Abuyama, Myoken, Yagi and Iwao—were mainly used for the determination of hypocenters. At these four stations, the seismographs of OB type with smoked-paper recorders are equipped from the beginning of the routine observation. On the other hand, at the other two stations—Kamigamo and Yagi—, seismic motions were being recorded by the seismographs of SH-II type with film recorders. The running speed of the film recorder (20mm/min) is slower than that of the smoked-paper recorder (120mm/min). Since the accuracy of time readings by means of the film recorder is inferior to that

by means of the smoked-paper recorder, the seismographs of OB type with smoked-paper recorders were equipped at Kamigamo- and Yagi station instead of the seismographs of SH-II type in March 1964 and October 1964 respectively. Since then, data of six observation stations have been much available for the analysis.

In this paper, the authors begin by giving an outline of a method of calculating hypocenter, origin time and velocity, and discuss in detail the distribution of epicenters and focal depths which are determined by use of data obtained after the publication of the first paper. The distributions of epicenters as well as of focal depths given in the present paper are more reliable than the distributions of the first paper, because the arrival times of four stations were mainly used for determining the hypocenters in the first paper. On the basis of the epicenters determined with reliable accuracy, the distribution of the first motions of P wave is also investigated for the purpose of making the focal mechanism of micro-earthquakes clear. Furthermore, comparative studies of the micro-earthquakes with the larger earthquakes are made from the view points of the distribution of epicenters and stress producing earthquakes. Finally, the mean velocity of the region concerned is estimated from the arrival times of P and the travel time curve of S.

## 2. Method of analysis

If the propagation velocity of P wave is assumed to be constant in the region concerned, the arrival time of P wave at each station satisfies the following equation:

$$(X_i - X)^2 + (Y_i - Y)^2 + (Z_i - Z)^2 = V^2(t_i - t)^2 \quad (1),$$

where  $(X_i, Y_i, Z_i)$  and  $(X, Y, Z)$  are the cartesian coordinates of the  $i$ -th station and hypocenter respectively, and  $V$  denotes the velocity of P wave,  $t_i$  the arrival time of the  $i$ -th station, and  $t$  the origin time.  $X$  and  $Y$  are measured positive eastward and northward respectively.  $Z$  is measured with respect to the sea level, and is positive downward.

Let us denote a first approximation solution of eq. (1) by  $X_0, Y_0, Z_0, t_0$  and  $V_0$ , and the error of the first approximation by  $\Delta X, \Delta Y, \Delta Z, \Delta t$  and  $\Delta V$ :

$$X = X_0 + \Delta X \text{ etc.} \quad (2).$$

$\Delta X$  etc. in eq. (2) are obtained by solving the normal equation of eq. (1). The normal equation is written in matrix notation as follows:

$${}^t\mathbf{A}\mathbf{A}\mathbf{A} = {}^t\mathbf{A}\mathbf{R} \quad (3),$$

where  $\Delta$  is a vector of which components are ( $\Delta X, \Delta Y, \Delta Z, \Delta t, \Delta V$ ),  $R$  a row vector of which components are the residuals of the stations, and the matrix  $A$  is

$$A = \begin{pmatrix} X_1 - X_0 & Y_1 - Y_0 & Z_1 - Z_0 & -V_0^2(t_1 - t_0) & V_0(t_1 - t_0)^2 \\ X_2 - X_0 & Y_2 - Y_0 & Z_2 - Z_0 & -V_0^2(t_2 - t_0) & V_0(t_2 - t_0)^2 \\ \dots & \dots & \dots & \dots & \dots \\ X_n - X_0 & Y_n - Y_0 & Z_n - Z_0 & -V_0^2(t_n - t_0) & V_0(t_n - t_0)^2 \end{pmatrix}.$$

${}^tA$  is the transpose matrix of  $A$ . In addition, the residual is expressed by

$$R_i = \{(X_i - X_0)^2 + (Y_i - Y_0)^2 + (Z_i - Z_0)^2 - V_0^2(t_i - t_0)^2\} / 2.$$

By use of eqs. (2) and (3), numerical calculations were carried out for the following two cases:

(a) *Calculation of hypocenter and origin time under the assumption that the propagation velocity of P wave is 5.5 km/sec and 6.0 km/sec in the region concerned.* In this case, the fifth row of  $A$  is unnecessary, because  $\Delta V$  vanishes. Thus,  ${}^tAA$  is a positive symmetric  $4 \times 4$  matrix, and eq. (3) gives four simultaneous equations for the four unknown deltas except  $\Delta V$ . The values of 5.5 km/sec and 6.0 km/sec were assigned to the velocity of P wave after the model of the crustal structure studied by the Research Group of Explosion Seismology (1961, Mikumo et al). In the first paper, the value of 5.0 km/sec was also assigned to the velocity of P. As discussed in §6, the mean velocity of P wave in the region concerned is probably more than 5.5 km/sec. Thus, the value of 5.0 km/sec was not used in the present paper.

(b) *Calculation of velocity, hypocenter and origin time.* In this case,  ${}^tAA$  is a positive symmetric  $5 \times 5$  matrix, and eq (3) gives five simultaneous equations for the five unknown deltas. This calculation was mainly purposed to estimate the mean velocity of the region concerned in the present paper. Numerical calculations of case (b) were carried out only for the earthquakes observed at six stations.

In both cases, the calculation precedes by solving (3) for the errors,\* substituting them into (2) to find new approximation and repeating this process until the errors become satisfactorily small. In the present paper, the ending condition is given as follows:

$$|\Delta X| + |\Delta Y| + |\Delta Z| \leq 2 \text{ km and } |\Delta t| \leq 0.2 \text{ sec.}$$

\* A first approximation which is necessary to solve the normal equation (3) were obtained by solving eq. (1) under the assumption that  $Z_i = 0$  and  $V = 5.0 \text{ km/sec}$  on the basis of arrival times of arbitrary four stations. This process is also programmed for KDC-I.

But, for saving time, the iterative processing was carried out within the limit of ten times. For most events, the errors satisfied the ending condition within ten times of iteration, so that the limitation of the number of times of iteration was not so important to the present calculation.

Numerical calculations were carried out by use of KDC-I computer.\*

### 3. Distribution of epicenters

Of micro-earthquakes occurring from the middle of March to the last of December in 1964, 151 events were located in the present study. 105 events of them were observed simultaneously at five stations from the middle of March to the middle of October. The remaining 46 events occurring after the last decade of October were observed simultaneously at six stations. Much more micro-earthquakes were observed at each station, and were used to obtain the frequency diagrams of P-S times.

The epicentral locations determined by use of the assumed values of 5.5 km/sec and 6.0 km/sec for the velocity of P wave are shown in Figs. 1a and 1b. There is no great difference between these figures. This means that the distribution of epicenters is not seriously affected by the assumed values of velocity.

It is found from Figs. 1a and 1b that the epicenters of micro-earthquakes were almost distributed in a belt-like region running from the west coast of Lake Biwa to Osaka Bay. The belt-like region has the width of about 25km. All the observation stations except Iwao station are included in this region. It is a matter of course that the locating of epicenter is influenced by the arrangement of the stations used for locating. It is, however, seen that micro-earthquakes occurring outside the net of the observation stations were not symmetrically distributed to the observation net; there were a large number of earthquakes to the north and to the south of the net, while there were only a few number of earthquakes to the east and to the south of the net. Especially micro-earthquakes did not occur to the west of the observation net. It may be concluded from these fact that the micro-earthquakes observed in the vicinity of Kyoto occur concentratedly in the belt-like region running from the west coast of Lake Biwa to Osaka Bay with the exception of a few number of earthquakes occurring to the southwest of Iwao station. By the way, the fact that there were no earthquakes to the west of the seismic active region is partly due to lack of observation station in a region to the west of the belt-like region. Whether micro-earthquakes occur or not will be made clearer if the routine observation start at the stations of Tan'nai and Tanto locating to the west of the belt-like region mentioned above.



Fig. 1a. Distribution of epicenters of the micro-earthquakes for the assumed velocity of 5.5 km/sec.

Fig. 1b. Distribution of epicenters of the micro-earthquakes for the assumed velocity of 6.0 km/sec.

In Figs. 1a and 1b, the epicentral locations are plotted by use of three marks (○, ◐ and ●). The marks represent the period of observation. The mark ○ correspond to the earthquakes observed from the middle of October in 1963 to the middle of March in 1964 at four stations, ◐ to the earthquakes observed at five stations from the middle of March to the middle of October in 1964, and ● to the earthquakes observed at six stations after the last of October. The epicenters marked by ○ were already determined in the first paper. It is easily found from Figs. 1a and 1b that the earthquakes were uniformly distributed in the belt-like region mentioned above without regard to the period of observation. This means that any significant variation of the places where micro-earthquakes occur with time were not found in about one and half years. Since the period of the observation is not so long, it is premature to conclude that there exist no variation of seismic active region with time.

Although any significant variation of seismic active region with time has not been found hitherto, it is often observed that a large number of micro-earthquakes concentratedly occurred in a small region within a short period, and that a large number of micro-earthquakes intermittently occurred in a small region. An example of concentrated occurrence was seen at Myoken station in May, 1964. Micro-earthquakes whose epicenters are guessed to lie to the west of Myoken occurred about hundred times per day. This occurrence lasted two days. Intermittent occurrence was seen, for an example, at Kamigamo station. Ten or more micro-earthquakes whose epicentral locations were

estimated to be a few km east away from Kamigamo repeatedly occurred for every other month in 1964.

Next we refer to the seismic activity of the larger earthquakes in and near the belt-like region mentioned above, and discuss the relation between micro-earthquakes and the larger earthquakes including destructive ones. Fig. 2 shows the distribution of earthquakes occurring from 1951 to 1964 in Kansai

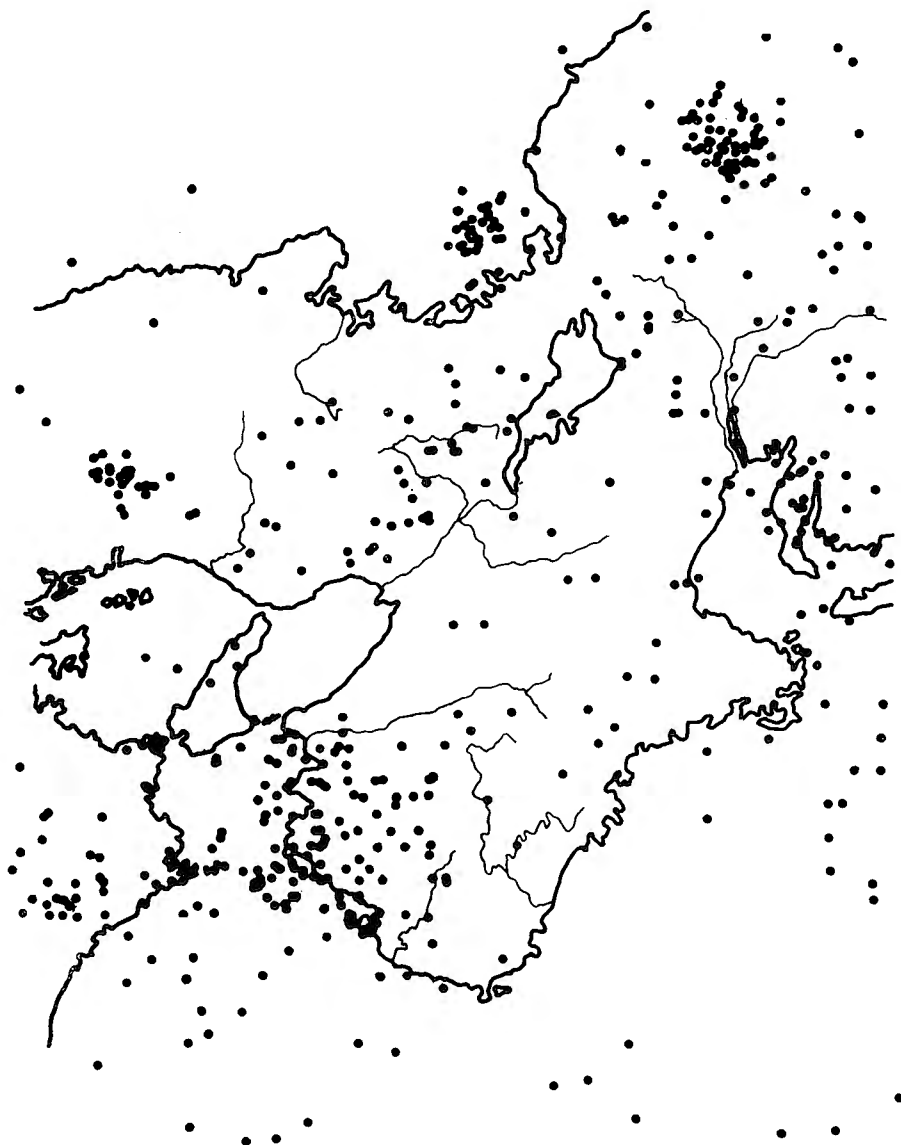


Fig. 2. Distribution of the earthquakes occurring from 1951 to 1964 in Kansai District (after Seismological Bulletin of J. M. O.)

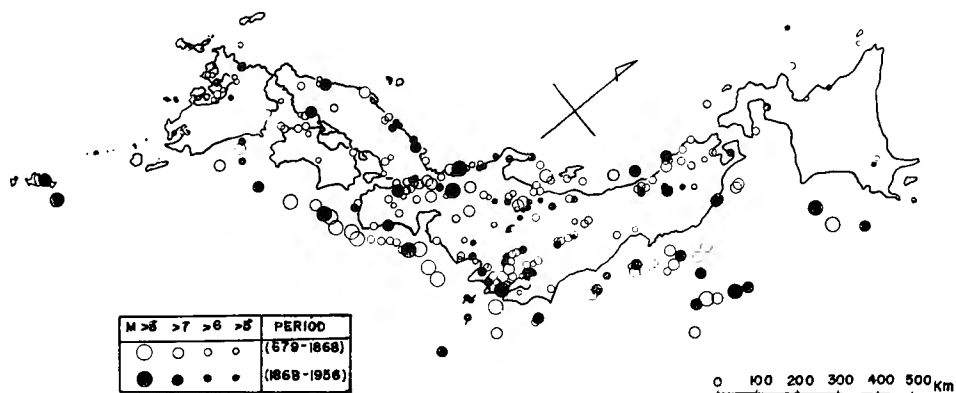


Fig. 3. Distribution of the destructive earthquakes on record (Muramatsu, 1965)

District. These earthquakes are plotted after the Seismological Bulletin of Japan Meteorological Agency. Thus the earthquakes shown in Fig. 2 are larger in magnitude than the micro-earthquakes treated in the present study. It is much interesting that the larger earthquakes as well as micro-earthquakes frequently occurred in the belt-like region mentioned above. It is also seen that the larger earthquakes scarcely occurred to the west of the belt-like region. Destructive earthquakes on record have been investigated by Kawasumi (1960), Muramatsu (1965) and others. In Fig. 3, the distribution of destructive earthquakes occurring from 679 to 1956 are reproduced from Muramatsu's recent paper. It is easily found from Fig. 3 that there were many destructive earthquakes in the belt-like region. It may be considered from these fact that earthquakes of various magnitudes are frequent in the belt-like region. The so-called "Yodogawa Seismic Zone" is considered to correspond to this seismic active belt-like region. For convenience, we call the belt-like region running from the west coast of Lake Biwa to Osaka Bay "Kyoto Seismic Zone" in the following. According to the map of destructive earthquakes shown by Muramatsu, destructive earthquakes were not so frequent in Wakayama District where micro-earthquakes are most frequent. Thus, a distinctive feature of "Kyoto Seismic Zone" is that destructive earthquakes as well as micro-earthquakes are frequent there. As discussed in § 5, the direction of the maximum pressure of the micro-earthquakes treated here agrees well with that of destructive earthquakes. Thus, the micro-earthquakes have close relation to the larger earthquakes from the view point of stress producing earthquakes in Kyoto Seismic Zone". We will discuss in detail in the later section.

#### 4. Distribution of focal depths

The focal depths of the micro-earthquakes are shown in Figs. 4 and 5.

In fig. 4, the hypocenters of the micro-earthquakes are plotted in a vertical section perpendicular to the line that links Abuyama- with Myoken station. The upper figure shows the distribution of depths for the assumed velocity of 5.5 km/sec, and the lower one the distribution of focal depths for 6.0 km/sec. The marks  $\circ$ ,  $\odot$  and  $\bullet$  represent the same as those in Figs. 1a and 1b.

The distribution of focal depths depends more strongly on the assumed values of velocity of P wave than the distribution of epicenters. As shown by Fig. 4, the focal depths are a little deeper for the assumed value of 5.5 km/sec than for the assumed value of 6.0 km/sec. It is, however, seen that the general tendency of the distribution of focal depths is not seriously affected by the assumed velocity.

According to the crustal structure of Kinki District proposed by the Rese-

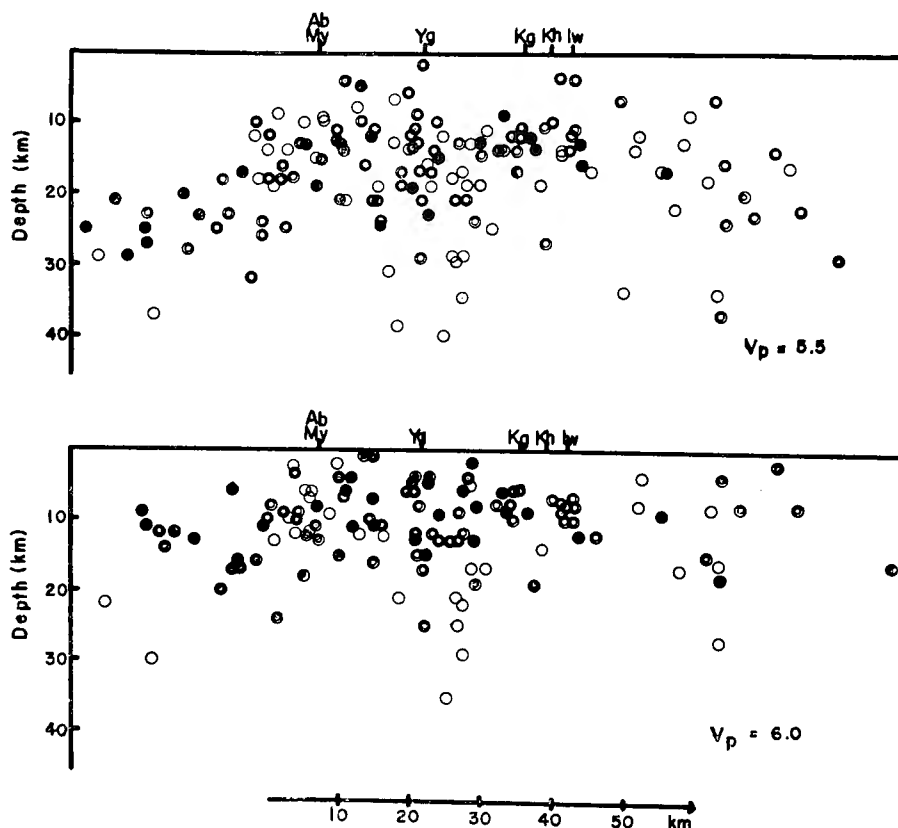


Fig. 4. Distribution of the focal depths of micro-earthquakes in a vertical section parallel to the belt-like seismic active region.



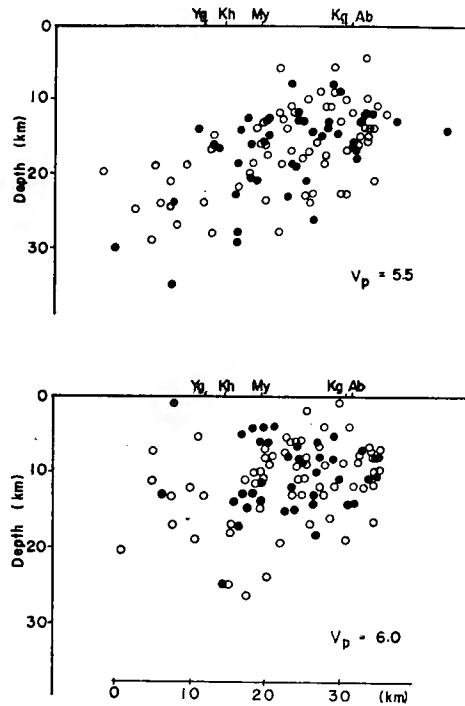


Fig. 5. Distribution of the focal depths of micro-earthquakes in a vertical section perpendicular to the belt-like seismic active region.

arch Group for Explosion Seismology, the crustal structure of "Kyoto Seismic Zone" may be approximated by two layered structures; the velocity of P wave for the upper layer is 5.5 km/sec, and that for the lower layer is 6.0 km/sec. Therefore, it is reasonable to consider that the focal depth of the earthquakes occurring in the lower layer closely approximates to the depth calculated by use of the assumed velocity of 6.0 km/sec. The deepest of focal depths calculated by use of 6.0 km/sec is, as shown in Figs. 4 and 5, about 35 km. The thickness of the crust of Kinki District is also about 35 km according to the study of the Research Group for Explosion Seismology. It follows that the micro-earthquakes in "Kyoto Seismic Zone" have their foci within the crust. As stated in § 6, the mean velocity of P wave in the region concerned, if uniform, is calculated to be about 5.8 km/sec. Furthermore, according to the analysis of the travel time of S wave, as discussed also in § 6, the value of 6.0 km/sec is better than the value of 5.5 km/sec for the velocity of P wave. Therefore, the distribution of focal depths for the assumed velocity of 6.0 km/sec is more probable than that for 5.5 km/sec.

In Fig. 5, the hypocenters of the micro-earthquakes are plotted in the

vertical section passing through Abuyama- and Myoken station. This section crosses perpendicularly to the vertical section used in Fig. 4. The upper figure shows the distribution of depths for the assumed velocity of 5.5 km/sec, and the lower one the distribution for the assumed velocity of 6.6 km/sec. The focal depths marked by ○ correspond to the earthquakes occurring from the middle of March to the middle of October in 1964, and ones marked by ● to the earthquakes occurring after the last of October in 1964.

According to Fig. 5, the micro-earthquakes locating in the east of "Kyoto Seismic Zone" have shallow foci, while those in the west have deep foci. It is seen that focal depths become deeper toward the west end of the seismic active zone. This interesting feature can be found in the frequency diagrams of P-S duration times shown in Fig. 6. All observed earthquakes with P-S times of less than 9 sec, which include 151 earthquakes used for the determination of hypocenters, were used for constructing the frequency diagrams of P-S times. It is easily found from Fig. 6 that the micro-earthquakes ob-

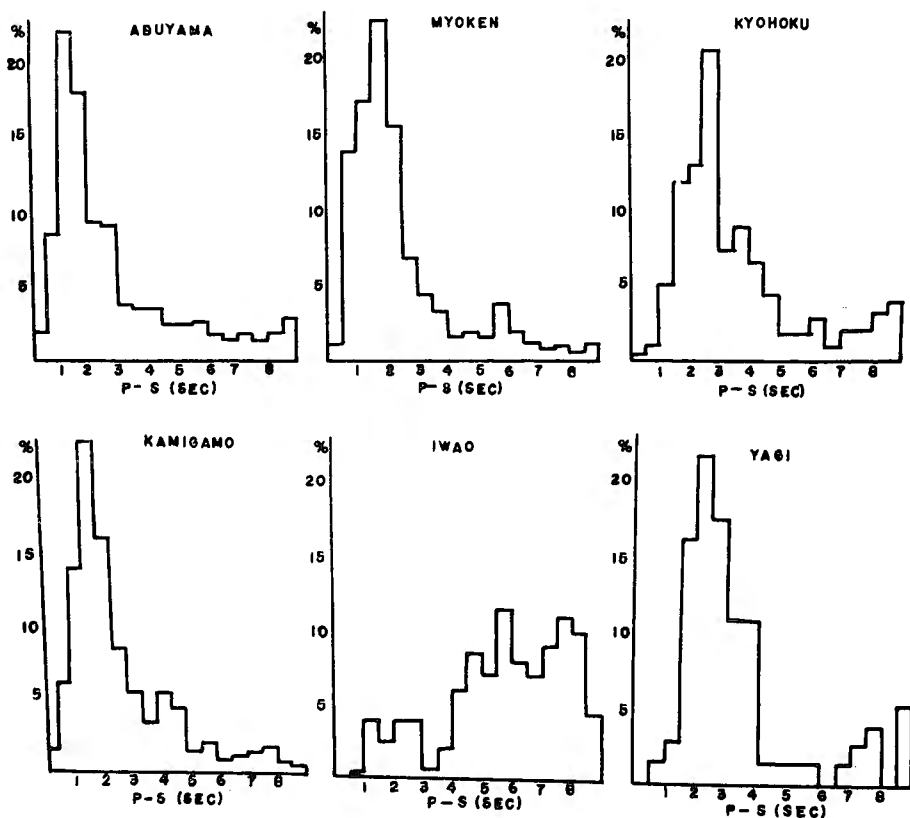


Fig. 6. Frequency diagram of the P-S duration times.

served at Abuyama- and Kamigamo station have comparatively shorter P-S times (0.5 to 3.0 sec) than those observed at Kyohoku and Yagi (1 to 4.0 sec). Abuyama and Kamigamo locate in the east of "Kyoto Seismic Zone", while Kyohoku and Yagi locate in the west. It is difficult to explain the difference between the P-S times of Abuyama- and Kamigamo station and those of Kyohoku- and Yagi station from the view point of the distribution of epicenters shown in Figs. 1a and 1b. The difference of P-S times may result from the fact that the focal depths of micro-earthquakes locating in the east of the seismic zone are shallower than those in the west.

#### 5. Distribution of the first motions of P wave and some geological features related to the seismic active zone

For the purpose of approaching the focal mechanism of the micro-earthquakes treated here, the first motions of P waves were examined. The seismographs used in our observation are almost of vertical type. Thus, we mainly concerned the distribution of condensational- and rarefactional waves. Since the number of observation stations are six in all, it is very difficult to decide a pattern of the distribution of the first motions for respective earthquake. Therefore, a pattern of the distribution of the first signs was decided by means of superposing the epicenters of all earthquakes. To be more precise, for all earthquakes of which epicenters were determined, the first signs of vertical components were so plotted in a single map that the epicenters of all earthquakes were displaced at the same location. The distribution of condensation and rarefaction thus obtained is shown in Fig. 7, where condensation is denoted by ●, and rarefaction by ○.

It is easily found from Fig. 7 that the whole region concerned is clearly divided into four quadrants by two nodal lines crossing perpendicularly each other at the superposed epicenter. One of the nodal lines runs from NE to SW, and another from NW to SE. It may be concluded from Fig. 7 that the distribution of the first motions of the micro-earthquakes treated here is of quadrant type.

The first motions of P waves are, as is shown in Fig. 7, rarefactional in the east- and the west quadrant, and condensational in the other quadrants. Therefore, the horizontal component of the maximum pressure of the micro-earthquakes can be considered to lie in the E-W direction. The horizontal component of the maximum pressure of very shallow earthquakes occurring in Kinki District lies in the ENE-WSW direction (1952, Honda). It is interesting that the direction of the maximum pressure of the micro-earthquakes agrees comparatively well with that of very shallow earthquakes which are larger in

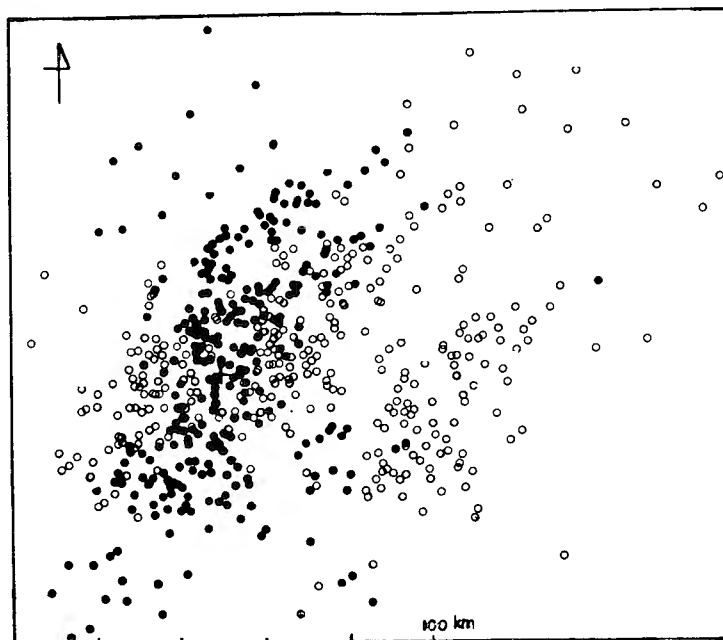


Fig. 7. The first motions of P waves of the micro-earthquakes, ●; condensation, ○; rarefaction, +; epicenter.

magnitude than the micro-earthquakes. This fact seems to suggest that stress producing earthquake in the region concerned is caused by the same focal mechanism regardless of magnitude. Whether the force acting the focus is now being studied by use of the first motions of S waves observed by the seismographs of horizontal type equipped at Abuyama Seismological Observatory.

It is made clear from the facts stated thus far that not only microearthquakes but the larger earthquakes including destructive ones are frequent in the belt-like seismic active region running from the west coast of Lake Biwa to Osaka Bay, and that stress producing earthquakes in the seismic region may be independent of their magnitude. Next, we refer to the geologically distinctive features related to this seismic region, and discuss their relation to the occurrence of the earthquakes.

One of the distinctive features is seen in the distribution of the Bouguer anomaly. In Fig. 8, the regions where the gradient of Bouguer anomaly is especially large are reproduced from Tsuboi's paper (1961). As is known from this figure, the present seismic active region belongs to the region where Bouguer anomaly changes remarkably. According to Tsuboi, remarkable- and rather remarkable earthquakes in Southwest Japan are frequent in the regions

where the gradient of Bouguer anomaly is large. This is true of the micro-earthquakes in this seismic region.

In Fig. 9 is shown the distribution of the horizontal displacements after Inoue (1960). It is easily found from this figure that the horizontal displacements are the smallest in the present seismic active region. In other words, the seismic active region is distinguished by the minimum displacements from the neighbouring regions. As for the neighbouring regions, the northeast part of Honshu is so displaced horizontally that it is bended convexly toward the Sea of Japan, and the southwest part of Honshu concavely toward the Sea of Japan. The seismic active region corresponds to a transitional zone from the region characterized by the convex bending to the region by the concave bending. It might be considered that the frequent occurrence of earthquakes seen in the present seismic region has some relation to the tectonic force which is suspected to be produced in the transitional zone owing to the different bendings of the neighbouring regions.

In Fig. 10, the distribution of Quaternary faults in Kinki District is shown after Hatori et al (1964). It is seen that there exist many faults in the seismic active region. The direction of the largest fault named Hanaore Fault agrees comparatively well with that of the nodal line running from NE to SW. Furthermore, there are some faults of which directions agree comparatively well with those of the nodal line running from NW to SE. Although these faults are not all active ones, the agreement of their directions with the nodal lines

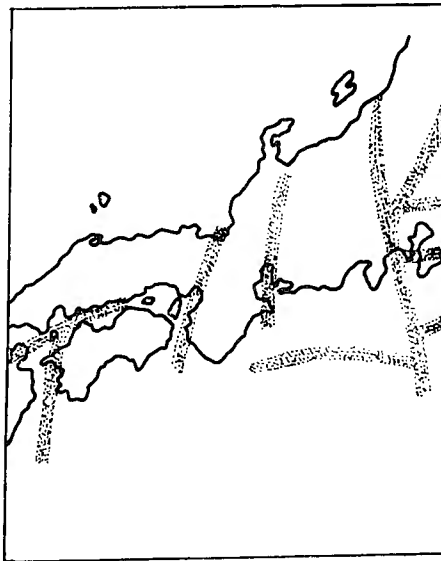


Fig. 8. Regions where the gradient of Bouguer anomaly is large (Tsuboi, 1961).

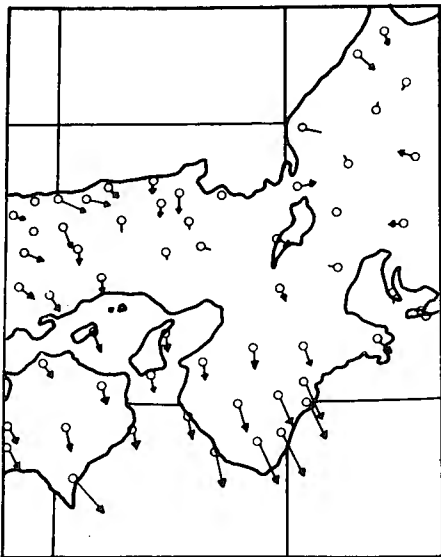


Fig. 9. Distribution of the horizontal deformation (Inoue, 1960).

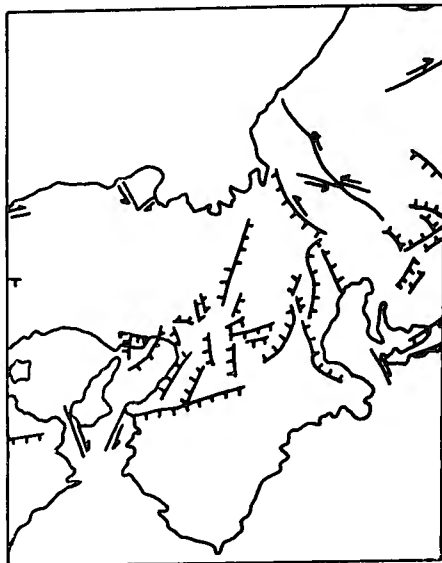


Fig. 10. Distribution of Quaternary faults (Hatori et al, 1964).

is suggestive to consider the relation of focal mechanism to fault. The relation between the focal mechanism and the faults will be studied by use of data of S wave in the following paper.

## 6. Estimation of the mean velocities of P and S wave

The epicentral locations and the focal depths which were shown in § 3 and in § 4 respectively were calculated, as stated before, under the assumption that the region concerned consists of a uniform layer with P velocity of 5.5 km/sec or 6.0 km/sec. Since the arrival times of more than four stations are available in the present study, we also calculated not only the hypocenters but the mean velocity of P wave (cf. (b) in § 2). A part of the calculation results is shown in Table. This calculation was mainly purposed to estimate the propagation velocity of P in the present paper, so that the distributions of epicenters and focal depths are not discussed in detail. However, we only point out that the distribution of epicenters is not significantly different from the distributions shown in Figs. 1a and 1b.

According to the present calculation, the mean velocity of P wave was estimated to be about 5.8 km/sec. This is the arithmetical mean value of velocities which were calculated by use of the arrival times of the earthquakes observed at six stations. The value of 5.8 km/sec for the mean value of P velocity is also supported from the consideration of the travel time curves of

Table. Part of the calculations by (b). Results for the micro-earthquakes occurring from Nov. 01 to Nov. 15 are illustrated.

## ORIGIN TIME, FOCUS AND VELOCITY

NO.	MTH	DT	H	M	S	X (KM)	Y (KM)	Z (KM)	V (K/S)
182	NOV	01	06	06	59.50	+21.60	+33.53	+ 0.18	+ 6.37
183	NOV	02	05	20	00.37	+ 7.08	- 0.33	+11.08	+ 5.19
184	NOV	02	13	47	53.02	- 7.45	-21.22	+16.52	+ 5.85
185	NOV	04	23	11	41.88	-26.34	-15.25	+11.46	+ 6.02
186	NOV	05	03	15	43.91	+10.28	+ 6.43	+ 6.69	+ 6.59
187	NOV	08	00	35	47.71	+20.07	+ 9.80	+26.87	+ 3.97
188	NOV	08	08	12	30.91	+ 8.45	+ 4.07	- 6.11	+ 7.14
189	NOV	08	13	14	40.72	- 2.65	-21.10	+48.87	+ 3.28
190	NOV	10	15	03	41.58	- 2.19	- 3.27	+ 1.17	+ 6.31
191	NOV	13	06	55	22.81	+ 5.72	- 2.87	- 2.80	+ 5.98
192	NOV	15	10	57	14.83	+ 4.26	+ 3.76	+ 7.40	+ 6.45
193	NOV	15	15	39	15.89	+11.33	-13.02	+ 0.29	+ 6.87
194	NOV	15	15	24	37.44	-15.30	+13.10	+17.67	+ 5.85

S wave.

The travel time curves of S waves are shown in Figs. 11a and 11b. These figures were drawn by use of the travel times of S waves on the basis of the

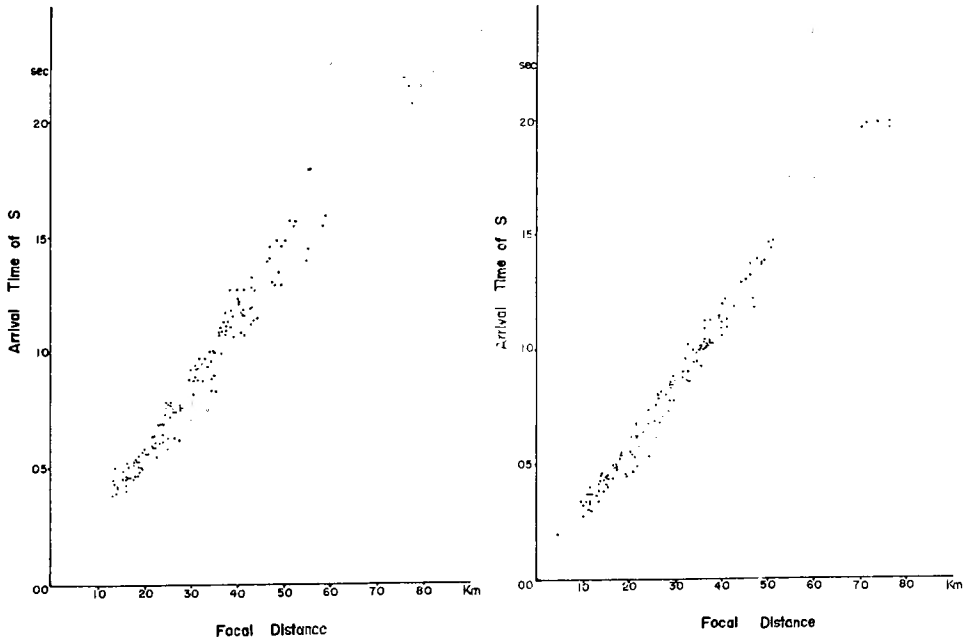


Fig. 11a. Travel time curves of S waves for the micro-earthquakes observed at five stations.

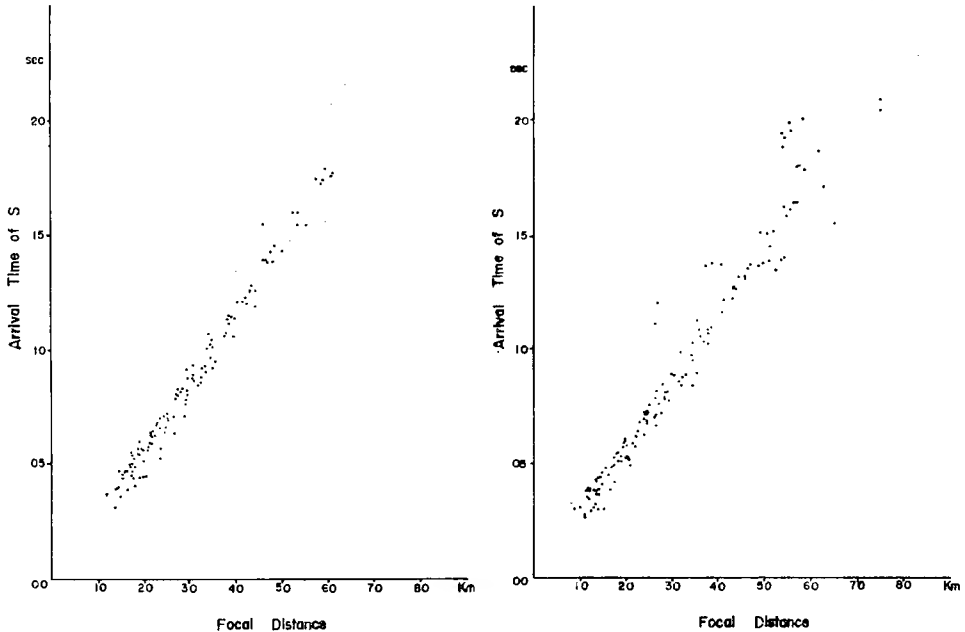


Fig. 11b. Travel time curves of S waves for the micro-earthquakes observed at six stations.

calculated values of the origin times and of the hypocentral distances for the assumed P velocities of 5.5 km/sec and 6.0 km/sec respectively. Figs. 11a and Figs. 11b correspond to the case that the number of the observation stations are 5 and 6 respectively; the left figure and the right one in each figure correspond to the velocity of 5.5 km/sec and 6.0 km/sec respectively.

As is known from Figs. 11a and 11b, the scattering of the travel times of S waves is less remarkable in the right figures than in the left figures. This means that the velocity of P wave of the region concerned is approximated better by 6.0 km/sec than by 5.5 km/sec. It is seen that the scatterings of the travel times of S waves become large at distances of more than 30 to 35 km. The distance of 30 to 35 km is a little larger than the diameter of a circle including the observation stations except Iwao station. For earthquakes occurring far away from the net of the observation stations, it is difficult to solve eq. (1) with reliable accuracy. In fact, the travel time curves of S waves are seemed to be inflected upward at distances of more than 40 km. This is probably due to not only the inaccuracy of the solutions but the assumption of uniform layer.

The velocity of S wave can be estimated from the gradient of the travel



time curve of S. It is found from Figs. 11a and 11b that the gradient of the travel time curves may be regarded as constant at distances of less than 35 to 40 km. The least square method being applied to the travel times at distances of less than 40 km, the velocity of S wave was calculated to range from 3.2 km/sec (corresponding to the case of  $V_p=5.5$  km/sec) to 3.5 km/sec (corresponding to the case of  $V_p=6.0$  km/sec).

It is reasonable to assume that the region concerned, if uniform, has the mean velocity of 5.8 to 6.0 km/sec for P wave, and the mean velocity of 3.4 to 3.5 km/sec for S wave. In particular, the velocity of P wave is compatible to the results obtained by the Research Group of Explosion Seismology.

## 7. Summary

The main results obtained in the present paper are summarized in the followings.

1. There exist a seismic active zone in the belt-like region running from the west coast of Lake Biwa to Osaka Bay with width of 25 km. In this region, not only micro-earthquakes but the larger earthquakes including destructive ones are frequent.

2. The focal depths of the micro-earthquakes occurring in the seismic active zone lie in the crust. The micro-earthquakes locating in the east part of the seismic zone have shallow foci, while these in the west part have deep foci.

3. The distribution of the first motions of P waves for the micro-earthquakes treated here is of quadrant type. The nodal lines cross perpendicularly each other at the epicenter; one of the nodal lines runs from NE to SW, and another from NW to SE. The first motions of P waves are condensational in the north- and the south quadrant, and rarefactional in the east- and the west quadrant. Therefore, the horizontal component of the maximum pressure lies in the E-W direction. The direction of the maximum pressure agrees comparatively well with that of very shallow earthquakes occurring in this seismic active region. This seems to suggest that stress producing earthquakes in the seismic active region is caused by the same focal mechanism regardless of magnitude.

4. The seismic active region is geologically characterized of the followings.

- (a) The gradient of Bouguer anomaly is especially large in this region.

- (b) The seismic active regions distinguished by the minimum horizontal displacements from the neighbouring regions.

- (c) There exist many Quaternary active faults in the seismic active region,

some of which lie in the same direction as the direction of the nodal lines.

5. The seismic active region has the mean velocity of 5.8 to 6.0 km/sec for P waves, and 3.4 to 3.5 km/sec for S wave according to the calculation under the assumption of uniform layer.

### References

- Hatori, K., S. Kaizuka, Y. Naruse, Y. Ota, A. Sugimura and T. Yoshinaka, 1964; Quaternary tectonic map of Japan (A preliminary note), Jour. Geod. Soc. Japan, 3-4, 111-115.
- Honda, H., 1954; "The seismic waves", (in Japanese), Iwanami.
- Inoue, E., 1960; Land deformation in Japan, Bull. Geograph. Survey Inst., 6, part 2-3, 73-134.
- Kawasumi, H., 1960; "Chronological Table of Science", (in Japanese), Tokyo Astronomical Observatory.
- Mikumo, T., M. Otsuka, T. Utsu, T. Terashima and A. Okada, 1961; Crustal structure in central Japan as derived from the Miboro explosion-seismic observation (in Japanese), part 2, On the crustal structure, Zisin, Ser. 2, 14, 168-188.
- Muramatsu, I., 1965; "Symposium on Scientific Research for Natural Disaster" (in Japanese), II, 1965, p. 203.
- Okano, K. and I. Hirano, 1964; Micro-earthquakes occurring in the vicinity of Kyoto (1), Special Contribution, Geophys. Inst., Kyoto Univ., No. 4, 63-74.
- Tsuboi, C., 1961; "Chikyu no Kosei (Tsuboi, C., ed.)", Chap. VII, "Jishin", Iwanami, 163-192.